JBMR PLUS Open Access ASBMR

Cx43 Overexpression in Osteocytes Prevents Osteocyte Apoptosis and Preserves Cortical Bone Quality in Aging Mice

Hannah M Davis,[1] Mohammad W Aref,[1] Alexandra Aguilar-Perez,[1] Rafael Pacheco-Costa,[1] Kimberly Allen,[1] Sinai Valdez,[1] Carmen Herrera,[1] Emily G Atkinson,[1] Arwa Mohammad,[1] David Lopez,[1] Marie A Harris,[2] Stephen E Harris,[2] Matthew Allen,[1] Teresita Bellido,[1,3,4] and Lilian I Plotkin[1,4]

[1]Department of Anatomy and Cell Biology, Indiana University School of Medicine, Indianapolis, IN, USA
[2]The University of Texas Health Science Center at San Antonio, San Antonio, TX, USA
[3]Division of Endocrinology, Department of Internal Medicine,, Indiana University School of Medicine, Indianapolis, IN, USA
[4]Roudebush Veterans Administration Medical Center, Indianapolis, IN, USA

ABSTRACT

Young, skeletally mature mice lacking Cx43 in osteocytes exhibit increased osteocyte apoptosis and decreased bone strength, resembling the phenotype of old mice. Further, the expression of Cx43 in bone decreases with age, suggesting a contribution of reduced Cx43 levels to the age-related changes in the skeleton. We report herein that Cx43 overexpression in osteocytes achieved by using the DMP1-8kb promoter ($Cx43^{OT}$ mice) attenuates the skeletal cortical but not trabecular bone phenotype of aged, 14-month-old mice. The percentage of Cx43-expressing osteocytes was higher in $Cx43^{OT}$ mice, whereas the percentage of Cx43-positive osteoblasts remained similar to wild-type (WT) littermate control mice. The percentage of apoptotic osteocytes and osteoblasts was increased in aged WT mice compared with skeletally mature, 6-month-old WT mice, and the percentage of apoptotic osteocytes, but not osteoblasts, was decreased in age-matched $Cx43^{OT}$ mice. Aged WT mice exhibited decreased bone formation and increased bone resorption as quantified by histomorphometric analysis and circulating markers compared with skeletally mature mice. Further, aged WT mice exhibited the expected decrease in bone biomechanical structural and material properties compared with young mice. Cx43 overexpression prevented the increase in osteoclasts and decrease in bone formation on the endocortical surfaces and the changes in circulating markers in the aged mice. Moreover, the ability of bone to resist damage was preserved in aged $Cx43^{OT}$ mice both at the structural and material level. All together, these findings suggest that increased Cx43 expression in osteocytes ameliorates age-induced cortical bone changes by preserving osteocyte viability and maintaining bone formation, leading to improved bone strength. © 2018 American Society for Bone and Mineral Research.

KEY WORDS: AGING; APOPTOSIS; CONNEXIN 43; OSTEOCYTE; GENETIC ANIMAL MODELS

Introduction

Advanced age is associated with skeletal fragility as a result of decreases in bone quantity and quality due to changes in the structural and material properties of bone.[1,2] Bone remodeling, a coordinated process critical for the maintenance of bone quality, occurs throughout life; however, the rate of bone turnover significantly decreases with advancing skeletal age.[3,4] Alterations in bone turnover where resorption outweighs formation eventually result in bone loss in old age. Initial age-induced bone loss is observed in trabecular bone due to decreased osteoblast activity, whereas cortical bone losses occur later.[5,6] In addition to the alterations in bone structure, bone material is also affected in aging,[5] as changes in bone mineral matrix and collagen composition as well as accumulation of microdamage further contribute to the increased skeletal fragility with aging.[2]

Numerous studies suggest that the extensive osteocyte network within the mineralized bone matrix plays an essential role in orchestrating bone remodeling through cell-cell communication among neighboring osteocytes and with cells on the bone surface.[7,8] Consistent with this notion, old age and conditions of increased skeletal fragility are associated with reductions in osteocyte viability and increased prevalence of empty lacunae, and disruptions in the osteocyte network alter osteocytic regulation of bone remodeling.[9] Osteocytes control intercellular signaling with distant cells both through the extracellular release of molecules and cytokines via hemichannels formed via connexins (Cx) and directly with adjacent cells through gap junction channels, formed by connexons

Received in original form December 21, 2017; revised form January 11, 2018; accepted January 16, 2018. Accepted manuscript online January 18, 2018.
Address correspondence to: Lilian I Plotkin, PhD, Department of Anatomy and Cell Biology, Indiana University School of Medicine, 635 Barnhill Drive, MS-5035, Indianapolis, IN 46202-5120, USA. E-mail: lplotkin@iupui.edu
Additional Supporting Information may be found in the online version of this article

JBMR® Plus, Vol. 02, No. xx, Month 2018, pp 1–11
DOI: 10.1002/jbm4.10035

present on the surface of neighboring cells.[10,11] Cx transmembrane proteins are expressed in osteoblasts, osteocytes, and osteoclasts, with Cx43 being the most highly expressed connexin in bone.(12)

The critical role of Cx43 in early and mature osteoblasts as well as in osteocytes has been demonstrated in numerous studies.[13–15] We previously showed that removal of Cx43 from osteocytes results in a skeletal phenotype that resembles that of aged mice with increased osteocyte apoptosis, enhanced osteoclast recruitment to bone surfaces, and defective bone material properties.[13,16] Further, Cx43 is significantly decreased in old mice and humans.[4,16] Overall, these findings demonstrate the essential role that Cx43 plays in maintaining osteocyte viability and bone homeostasis, thus underscoring the potential contribution of reduced levels of Cx43 in osteocytes to the bone weakness in aging. However, the specific role that osteocytic Cx43 plays in controlling bone structure and strength in aging has not been studied.

We investigated here whether expression of an osteocyte-targeted Cx43 transgene could preserve osteocyte viability and attenuate the skeletal phenotype in aged mice, using mice in which the DMP1-8kb promoter targeted Cx43 expression to osteocytes ($Cx43^{OT}$ mice). Overall, the results of this study demonstrate that increased osteocytic Cx43 expression partially preserves osteocyte viability and maintains cortical bone quality in aged mice. Because overexpression of Cx43 in osteocytes does not significantly affect cancellous bone, these findings also point to a site-specific effect of Cx43 in osteocytes.

Materials and Methods

Mice

DMP1-8kb-Cx43/GFP mice (abbreviated as $Cx43^{OT}$) were generated at the Transgenic and KO Mouse Core (IUSM) with the Cx43 transgene, generated by S and M Harris (UTSHC, San Antonio, TX, USA), using the DMP1-8kb promoter[17] CMV-Cx43/GFP[18] constructs (Supplemental Fig. S1*A*). The presence of the transgene was evaluated by PCR in genomic DNA extracted from ear notch samples using primer sets for Cx43 and GFP. DMP1-GFP mice were used as positive controls for GFP.[17] GFP expression in DNA from $Cx43^{OT}$ mice was detected by PCR but not by fluorescent microscopy, possibly because of low expression resulting from the transgene construct design in which GFP was after IRES.

All mice were maintained on a C57BL/6Nhsd background (Envigo, Indianapolis, IN, USA) and littermates were used as controls. Mice were fed a regular diet and water *ad libitum* and were maintained on a 12-hour light/dark cycle. Mice were born at the expected Mendelian frequency, were fertile, and exhibited a similar size and weight to wild-type (WT) littermate mice at birth. Female skeletally mature 6-month-old and aged 14-month-old mice were used. Based on published data, our 6-month-old mice are equivalent to 20-year-old humans, whereas the 14-month-old mice correspond to middle-aged humans at the end of their reproductive stage of life (approximately 58 years old).[19] For dynamic histomorphometric studies, mice received intraperitoneal injections of calcein (30 mg/kg) and alizarin red (50 mg/kg) (Sigma Chemical, St. Louis, MO, USA) 7 and 2 days before euthanization, as published.[20] The protocols involving animal procedures were approved by the Institutional Animal Care and Use Committee of Indiana University School of Medicine.

Osteoblast and osteocyte isolation

Calvaria cells were isolated from $Cx43^{OT}$ mice bred to DMP1-8kb-GFP mice, which have GFP-labeled osteocytes.[16,21] Cells were isolated by sequential 20-minute digestions using a trypsin/EDTA/collagenase P mixture as previously described.[22] The first digestion was discarded, and cells from all other digestions were pulled. GFP-expressing cells (osteocyte-enriched) were separated from GFP-negative cells (osteoblast-enriched) by sorting the cell suspension using a FACSAria flow cytometer (BD Biosciences, Sparks, MD, USA) at the Indiana University Flow Cytometry Core Facility, as published.[23]

RNA extraction and real-time PCR (qPCR)

Total RNA was isolated and purified using TRIzol (Invitrogen, Grand Island, NY, USA). Reverse transcription was performed using a high-capacity cDNA kit (Applied Biosystems, Foster City, CA, USA). qPCR was performed using the Gene Expression Assay Mix TaqMan Universal Master Mix containing 80 ng of each cDNA template using an ABI 7900HT real-time PCR system. The housekeeping gene glyceraldehyde 3-phosphate dehydrogenase (GAPDH) was used. Primers and probes were commercially available (Applied Biosystems) or were designed using the Assay Design Center (Roche Applied Science, Indianapolis, IN, USA). Relative expression was calculated using the ΔCt method.[23]

Immunohistochemistry

Cx43 expression in osteocytes and osteoblasts was visualized in paraffin-embedded femora from 2-month-old mice, as described.[23,24] Briefly, sections were deparaffinized, treated with 3% H_2O_2, blocked with rabbit serum, and incubated with 1:1000 anti-Cx43 (C6219) (Sigma-Aldrich, St. Louis, MO, USA). Sections were incubated with the corresponding biotinylated secondary antibody followed by avidin conjugated peroxidase (Vectastain Elite ABC Kit; Vectora Laboratories, Burlingame, CA, USA). Color was developed with a diaminobenzidine substrate chromogen system (Dako, Glostrup, Denmark). Sections were counterstained with 2% methyl green.[16] Cells expressing the protein are brown, whereas negative cells are green-blue. Non-immune IgGs were used as negative controls.

Western blotting analysis

Whole protein extracts from osteocyte-enriched long bones (cortical bone preparations), calvaria bones, and soft tissue samples were prepared as published.[16,25] Protein levels were measured by Western blot analysis. Membranes were probed with primary antibodies, rabbit anti-connexin43 (C6219), and mouse anti-β-actin (A5316) (Sigma-Aldrich) diluted 1:1000, overnight at 4°C, followed by incubation with corresponding secondary antibodies conjugated with horseradish peroxidase (Santa Cruz Biotechnology, Dallas, TX, USA) for 4 hours at room temperature. Membranes were developed with an enhanced chemiluminescence Western blotting substrate kit (Pierce Biotechnology Inc., Rockford, IL, USA). Bands were quantified using ImageJ.

Bone mineral density (BMD) by dual-energy X-ray absorptiometry (DXA)

BMD was measured monthly by DXA using a PIXImus densitometer (GE Medical Systems, Lunar Division, Madison, WI, USA).[20] BMD measurements included total BMD (excluding

the head and tail), entire femur (femoral BMD), and L_1 to L_6 vertebra (spinal BMD).[23] Calibration was performed before scanning with a standard phantom, as recommended by the manufacturer.

Apoptosis

Osteocyte and osteoblast apoptosis was detected in undecalcified vertebral bone sections and paraffin-embedded femur sections by TdT-mediated dUTP nick-end labeling (TUNEL) using a modified version of a commercial kit (EMD Millipore, Billerica, MA, USA) in sections counterstained with 2% methyl green, as published.[16]

Serum biochemistry

Plasma collected 3 hours after fasting by cheek bleeding was aliquoted and stored at −80°C.[20] N-terminal propeptide of type I procollagen (P1NP) (Immunodiagnostic Systems Inc., Fountain Hill, AZ, USA, cat. #AC-33F1) and C-telopeptide fragments (CTX) (RatLaps, Immunodiagnostic Systems Inc., cat. #AC-06F1) were measured as published.[16,26]

Micro-computed tomography (μCT) analysis

Femora and L_4 vertebrae were dissected, wrapped in saline-containing gauze, and frozen at −20°C.[26] Trabecular morphology of the L_4 vertebral body was obtained using the Skyscan 1172 system with a 60 kV source, 0.5 mm Al filter, 0.7 degree rotation, and two-image averaging with an isotropic voxel size of 6 μm.[27] Femora were scanned using a 55 kV source, 0.5 mm Al filter, 0.7 degree rotation, and two-image averaging with an isotropic voxel size of 9 μm using a SkyScan 1176 system (SkyScan, Kontich, Belgium). Scans were reconstructed and analyzed using manufacturer software. Two different systems were used because of constrained availability. Nomenclature is reported in accordance with suggested guidelines for μCT.[28]

Bone histomorphometry

Femora and vertebrae were dissected, fixed in 10% neutral-buffered formalin, and embedded in methyl methacrylate, as published.[26] Dynamic histomorphometric measurements were performed in unstained femoral mid-diaphysis and vertebrae sections.[26] Static histomorphometric analysis was performed on sequential plastic-embedded vertebra sections stained with von Kossa/McNeal for osteoblasts and TRAP/Toluidine blue for osteoclasts. Osteoclasts were also quantified on paraffin-embedded femur sections. Analysis was performed by blinded investigators using the OsteoMeasure high-resolution digital video system (OsteoMetrics Inc., Decatur, GA, USA).[25,29] The terminology and units used are those recommended by the Histomorphometry Nomenclature Committee of the ASBMR.[28]

Biomechanical testing

Three-point bending testing of the femoral mid-diaphysis was performed following previously published protocols.[26] Axial compression of the L_4 vertebrae was performed after removing the vertebral processes and endplates. A rate of 0.5 mm/min was used to load the vertebral bodies until failure, as previously described.[30] Structural mechanical properties were determined from the load-displacement curves using standard definitions, whereas material-level properties were derived from the load-displacement curves, cross-sectional moments of inertia, and the distances from the centroid to the tensile surface using geometrical data determined by μCT and standard beam-bending equations.[20]

Statistical analysis

Data were analyzed by using SigmaPlot (Systat Software Inc., San Jose, CA, USA). Differences were evaluated either by two-way ANOVA, with post hoc analysis using Tukey method or Student's *t* test, as appropriate. Differences were considered significant when $p < 0.05$.

Results

Effective expression of an osteocyte targeted Cx43 transgene in $Cx43^{OT}$mice

To test the effect of Cx43 levels on osteocyte viability and bone homeostasis in aged mice, we generated a transgenic mouse model that expresses a DMP1-8kb-Cx43/GFP transgene primarily in osteocytes ($Cx43^{OT}$ mice) (Supplemental Fig. S1*A*). An amplified fragment of 297 bp corresponding to the Cx43 allele and of 525 bp to the GFP allele was used to generate transgenic $Cx43^{OT}$mice. Of the 11 potential transgenic founders generated, two mice were found to express the exogenous Cx43 and GFP genes. Because of higher Cx43 protein levels in the founder mouse #82 (data not shown), offspring generated from this mouse were used for the outlined studies. Expression of both exogenous Cx43 and GFP were transmitted to half of the offspring when crossed with a WT mouse, as expected (Supplemental Fig. S1*B*). To confirm that our DMP1-8kb-Cx43/GFP transgene is primarily expressed in osteocytes and not in osteoblasts, $Cx43^{OT}$ mice were crossed with DMP1-8kb-GFP mice.[16,21] GFP-positive osteocytes (Ot) isolated by FACS expressed high levels of the osteocyte markers SOST, DMP1, and FGF23, whereas the osteoblast marker keratocan was low (Fig. 1*A*). GFP-negative osteoblasts (Ob) had undetectable levels of SOST and DMP1, whereas keratocan expression was higher, validating the identity of the cell populations. Cx43 expression was increased in the GFP-positive osteocytes and decreased in the GFP-negative osteoblasts isolated from $Cx43^{OT}$ compared with WT littermate mice, demonstrating osteocyte-specific expression of the transgene. Moreover, the percentage of Cx43-positive osteocytes, detected by Cx43 immunostaining, was increased twofold in $Cx43^{OT}$ mice compared with WT mice, whereas the percentage of Cx43-positive osteoblasts on the bone surface was similar, although it showed a tendency toward decrease (Fig. 1*B*), similar to the Cx43 mRNA levels in osteoblastic cells (Fig. 1*A*). Cx43 expression at the protein level, measured by Western blotting analysis, was not increased in marrow-flushed cortical bone preparations or in calvaria lysates (Fig. 1*C*), possibly because of the presence of other Cx43-expressing cells, such as osteoblasts.[16] Further, no changes in Cx43 protein were detected in the heart, kidney, brain, or skeletal muscle of $Cx43^{OT}$ mice compared with WT mice.

Similar to mice lacking osteocytic Cx43,[16] overexpression of osteocytic Cx43 in $Cx43^{OT}$ mice did not exhibit changes in BMD during growth in female (Fig. 1*D*) or male mice (data not shown), demonstrating that Cx43 in osteocytes is not involved in bone mass accrual. Total, femoral, and spinal BMD of the $Cx43^{OT}$ and WT mice by DXA were similar up to 5.5 months, except for a slight increase in total and femoral BMD in the female $Cx43^{OT}$ mice at age 2 months, which was consistent with reduced BMD at this age in mice lacking osteocytic Cx43.[16] No decreases in

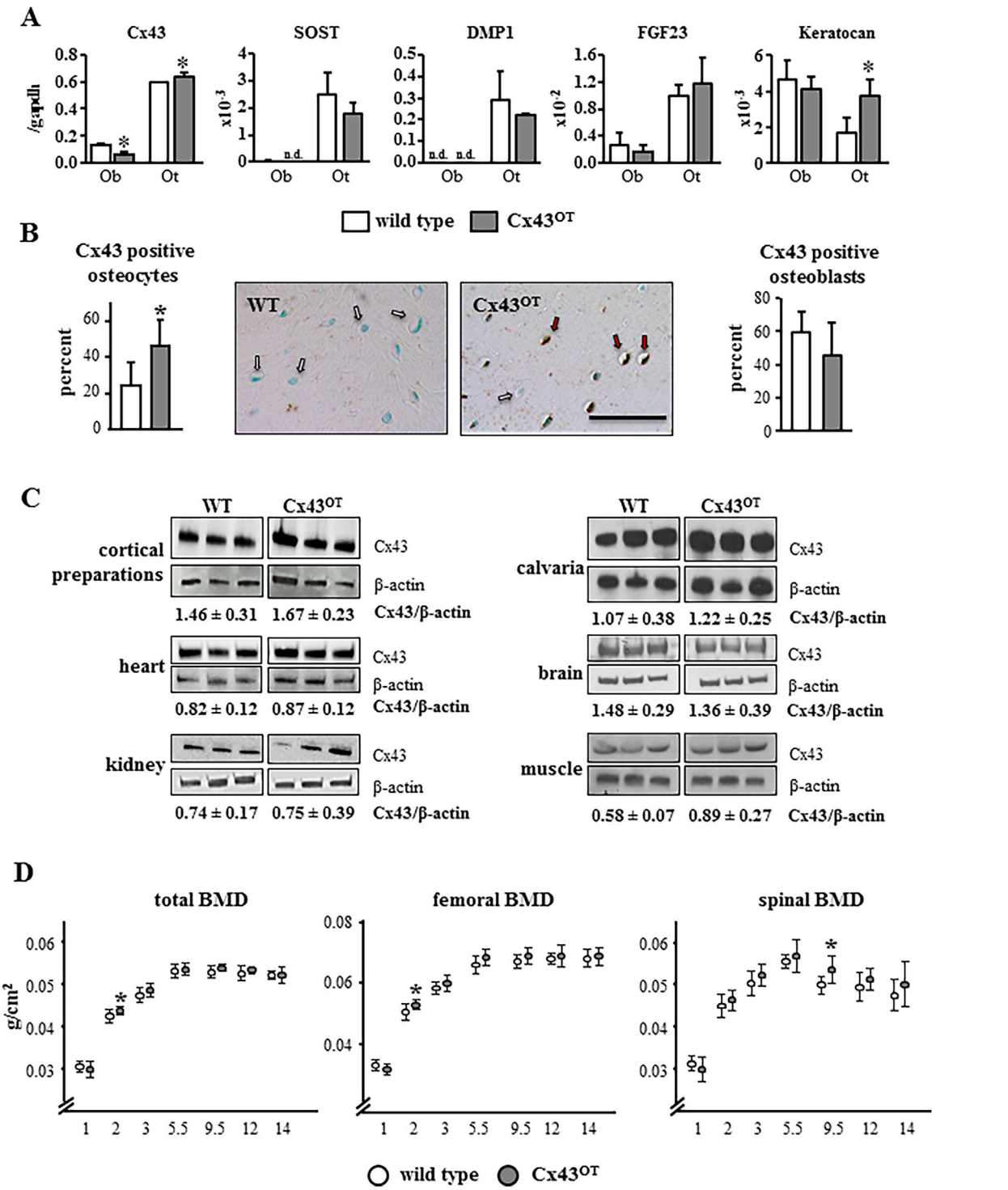

Fig. 1. Effective osteocyte targeted Cx43 transgene expression in DMP1-8kb-Cx43/GFP ($Cx43^{OT}$) mice. (*A*) mRNA expression in primary osteoblasts and osteocytes isolated from DMP1-8kb-GFP mice expressing GFP under the control of the 8-kb fragment of the DMP1 promoter. Ob = osteoblastic cells; Ot = osteocytic cells; n.d. = non-detectable. Bars represent mean ± SD of triplicate measurements, $^{*}p < 0.05$, *t* test versus WT cells. (*B*) Cx43 expression in osteocytes and osteoblasts was evaluated in the femoral mid-diaphysis of $Cx43^{OT}$ and WT littermate mice stained with a non-immune IgG or anti-Cx43 polyclonal antibody, counterstained with 0.2% methyl green. Bars represent mean ± SD, $^{*}p < 0.05$, *t* test versus WT mice, $n = 6$ WT and $n = 4$ $Cx43^{OT}$. Representative images of Cx43-negative (arrow, white) and Cx43-positive (arrow, red) osteocytes are shown. Scale bar = 25 μm. (*C*) Cx43 protein levels measured in marrow-flushed cortical bone preparations, calvarial bones, and in the soft tissues of $Cx43^{OT}$ and WT mice by Western blot correct by β-actin levels, $n = 3$. (*D*) Total body, spinal, and femoral BMD were measured from 1 to 14 months of age by DXA in females, $n = 13$ WT and $n = 11$ $Cx43^{OT}$. Symbols represent ± SD, $^{*}p < 0.05$ versus WT littermates by *t* test.

total or femoral BMD were observed in either genotype up to 14 months compared with 5.5-month-old mice. On the other hand, spinal BMD began to decline at 9.5 months in the WT mice, and by 12 months decreases in spinal BMD were detected in both genotypes.

Increased Cx43 expression reduces osteocyte apoptosis in aged mice

To investigate the effects of aging on osteocyte viability, apoptosis was quantified in the different bone compartments of the lumbar vertebra and femur. No changes in the percentage of apoptotic osteocytes or osteoblasts were detected between the two genotypes at 6 months of age (young mice) (Fig. 2*A*). Aged WT mice exhibited a 6- and 5.5-fold increase in osteocyte apoptosis in the cortical and cancellous vertebral bone, respectively, and a 22-fold increase in cancellous osteoblast apoptosis compared with young WT mice.[3,31] Cortical and cancellous osteocyte apoptosis was higher in aged compared with young animals even in Cx43^{OT} mice; however, osteocyte apoptosis was 40% lower in the cortical bone and 24% lower in the cancellous bone of the vertebra in the aged transgenic mice compared with WT mice. Similar decreases were detected in the femoral cortical bone of aged transgenic mice compared with WT mice (Fig. 2*B*). In contrast, the prevalence of apoptotic cancellous osteoblasts was increased approximately 40% with aging in both genotypes and no differences in osteoblast viability were detected between the two genotypes at 14 months of age (Fig. 2*A*). Thus, increased expression of Cx43 in osteocytes partially prevents the increase in osteocyte apoptosis induced by aging.

Endocortical bone formation is maintained in aged Cx43^{OT} mice

Aging led to alterations in the bone turnover markers in the WT mice, with a 42% decrease in the formation marker P1NP and a 34% increase in the resorption marker CTX in aged compared with young WT mice (Fig. 3*A*). On the other hand, P1NP levels were increased 66% and CTX levels were decreased 24% in aged compared with young Cx43^{OT} mice. Moreover, although no changes in P1NP were detected between the two genotypes in young mice, aged Cx43^{OT} mice exhibited 135% higher P1NP levels compared with WT mice of the same age. Further, at 6 months of age, CTX levels were slightly increased in the Cx43^{OT}

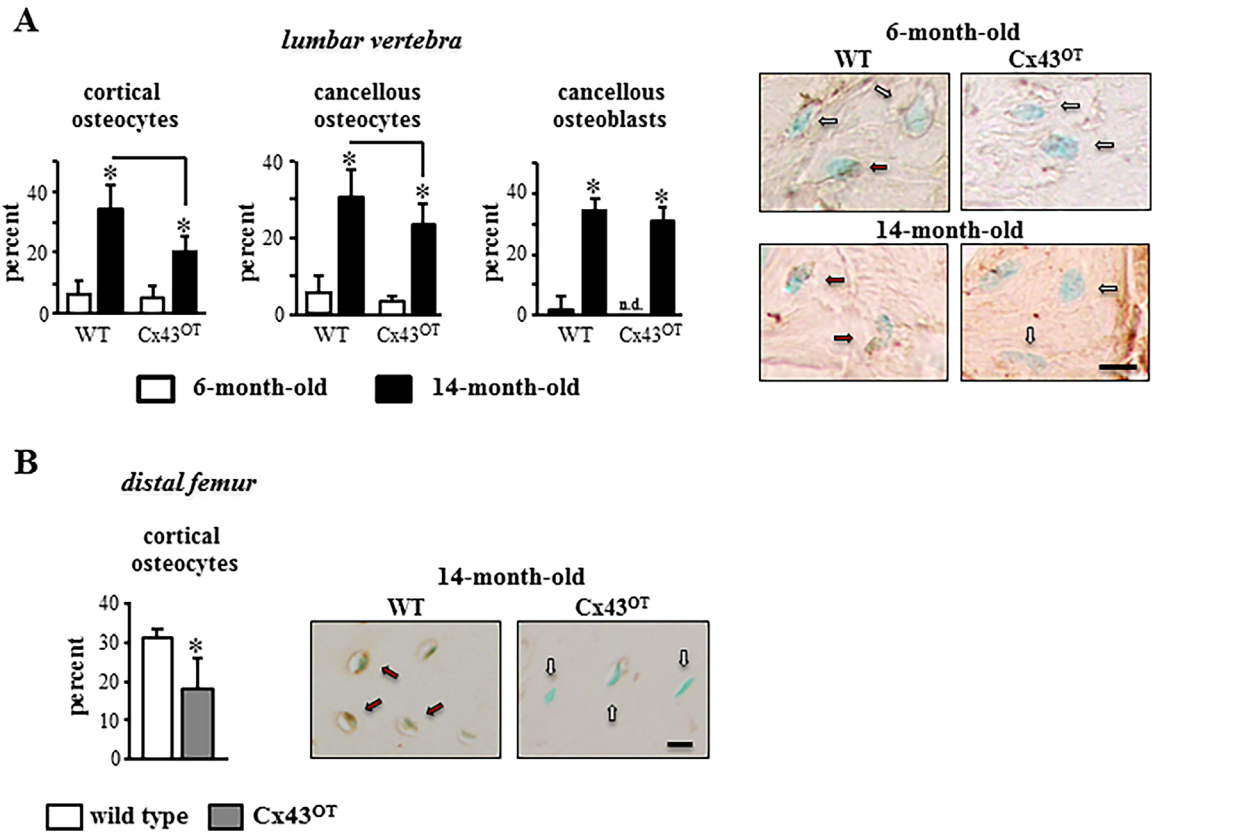

Fig. 2. Expression of Cx43 in osteocytes reduces osteocyte apoptosis induced with aging. (*A*) Percentage of apoptotic (TUNEL-positive) cortical and cancellous osteocytes, as well as cancellous osteoblasts were scored in vertebral bone sections. Bars represent mean ± SD, $^{*}p < 0.05$, versus 6-month-old genotype-matched mice by two-way ANOVA, Tukey, black line: $p < 0.05$, versus old control mice by *t* test. Six-month-old mice: $n = 9$ WT and $n = 8$ Cx43^{OT}, 14-month-old mice: $n = 8$ WT and $n = 7$ Cx43^{OT}. Representative images of TUNEL-negative (arrow, white) and positive (arrow, red) osteocytes are shown. Scale bar = 2.5 μm. (*B*) Percentage of apoptotic cortical osteocytes were scored in longitudinal distal femur sections from 14-month old mice. Bars represent mean ± SD, $^{*}p < 0.05$ versus WT littermates by *t* test, $n = 7$ WT and $n = 9$ Cx43^{OT}. Representative images of TUNEL-negative (arrow, white) and positive (arrow, red) osteocytes are shown. Scale bar = 6.25 μm.

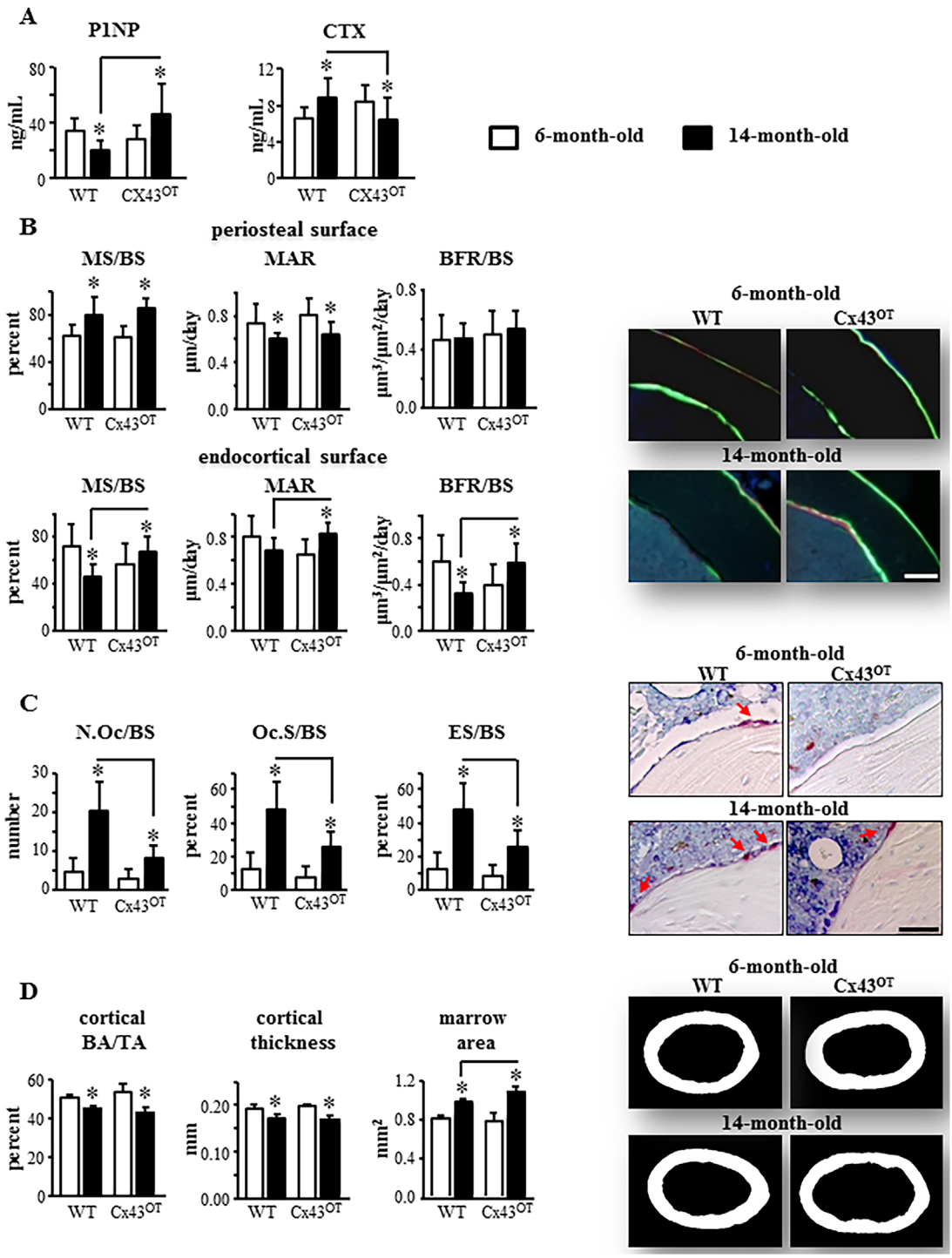

Fig. 3. Fourteen-month-old Cx43^{OT} mice exhibit enhanced endocortical bone formation and decreased resorption. (*A*) Circulating levels for P1NP and CTX were measured by ELISA in serum collected from 6- and 14-month-old mice. Six-month-old mice: $n = 10$ WT and $n = 9$ Cx43^{OT}, 14-month-old mice: $n = 11$ WT and $n = 9$ Cx43^{OT}. (*B*) Periosteal and endosteal MS/BS, MAR, and BFR/BS were measured in unstained sections from the femoral mid-diaphysis. Six-month-old mice: $n = 9$ WT and $n = 9$ Cx43^{OT}, 14-month-old mice: $n = 8$ WT and $n = 7$ Cx43^{OT}. Representative images are shown. Scale bars = 100 µm. (*C*) N.Oc/BS, Oc.S/BS, ES/BS were scored in femoral cortical mid-diaphysis after staining for TRAP/Toluidine blue in Cx43^{OT} and WT mice. Six-month-old mice: $n = 9$ WT and $n = 9$ Cx43^{OT}, 14-month-old mice: $n = 5$ WT and $n = 7$ Cx43^{OT}. Osteoclasts on the bone surface (arrow, red) are shown. (*D*) Cortical bone geometry was evaluated by µCT in the femoral mid-diaphysis. Six-month-old mice: $n = 8$ WT and $n = 9$ Cx43^{OT}, 14-month-old mice: $n = 8$ WT and $n = 6$ Cx43^{OT}. Representative reconstructed images of the femoral mid-diaphysis are shown. Bars represent mean ± SD, $^{*}p < 0.05$, versus 6-month-old genotype-matched mice by two-way ANOVA, Tukey, black line: $p < 0.05$, versus old control mice by *t* test.

mice, whereas at 14 months CTX levels were 28% lower compared with aged WT mice.

No changes in periosteal bone formation parameters, mineralizing surface per bone surface (MS/BS), mineral apposition rate (MAR), or bone formation rate per bone surface (BFR/BS), were detected between the two genotypes at either age in the femoral mid-diaphysis (Fig. 3*B*). On the other hand, dynamic histomorphometric analysis revealed that all bone formation indexes were increased on the endocortical surface in the Cx43^{OT} versus WT mice at 14 months but not at 6 months (Fig. 3*B*), consistent with the increased P1NP levels observed in the 14-month-old Cx43^{OT} mice. As for MS/BS, the surfaces occupied by single and double labels on the periosteum were similarly increased by aging independently of the genotype of the mice, whereas Cx43 overexpression did not alter these parameters (Supplemental Fig. S2*A*). On the other hand, the percent single-labeled surface on the endocortex was increased by aging and decreased by the transgene, whereas double-labeled-covered surface was decreased in 14-month-old wild-type mice but increased in Cx43^{OT} mice compared with the corresponding 6-month-old mice (Supplemental Fig. S2*B*).

Further, similar to the decreases in CTX observed in the Cx43^{OT} mice at 14 months of age, static histomorphometric analysis of the endocortical surface of the femoral mid-diaphysis revealed a 2.5-fold reduction in the number of osteoclasts per bone surface (N.Oc/BS), a 1.9-fold decrease in bone surface occupied by osteoclasts (Oc.S/BS), and a 1.9-fold reduction in the eroded bone surface (ES/BS) in the 14-month-old Cx43^{OT} compared with WT mice (Fig. 3*C*).

Cortical bone mechanical properties are preserved in aged Cx43^{OT} mice

μCT analysis revealed that both WT and Cx43^{OT} mice exhibited the expected age-related skeletal alterations in cortical bone geometry of the femoral mid-diaphysis, with increased marrow cavity area, as well as decreased cortical thickness (Ct.Th) and bone area/tissue area (BA/TA) in aged mice (Fig. 3*D*). Further, we did not detect changes in the cortical bone geometry of the femur between the genotypes at either age, aside from a slight increase in marrow cavity area of the aged Cx43^{OT} mice.

In contrast, biomechanical studies of the femur by 3-point bending revealed that increased osteocytic Cx43 expression enhanced the structural and material bone properties in skeletally mature mice and prevented the loss of these properties in aged mice (Fig. 4). At 6 months of age, Cx43^{OT} mice exhibited enhanced femoral structural properties with increased yield force, ultimate force, stiffness, and work to yield (Fig. 4*A*), as well as increases in the material properties yield stress, modulus, and resilience (Fig. 4*B*). Moreover, aging in the WT mice resulted in decreases in both the structural and material properties of the femoral bone, with decreases in ultimate force/stress, stiffness/modulus, postyield/total work, and toughness. Further, decreases were detected in the pre-yield properties with lower yield force/stress of WT bones from aged compared with young mice. In contrast, although decreases were detected in ultimate force/stress and stiffness/modulus of the femur from 14-month-old Cx43^{OT} mice, displacement/strain to yield were significantly increased compared with 6-month-old transgenic mice. Aged Cx43^{OT} mice also exhibited increases in the pre-yield properties, yield force/stress, displacement/strain to yield, and work to yield/resilience compared with WT mice at the same age. In contrast to the effects of osteocytic Cx43 overexpression on pre-yield properties, osteocytic Cx43 deletion results in reductions in the pre-yield properties of the cortical bone at both the structural and material level (Supplemental Table S1). Taken together, our data suggest that overexpression of osteocytic Cx43 in aging preserves certain cortical bone mechanical properties, maintaining the ability of the bone to absorb energy without damaging.

Increased osteocytic Cx43 does not prevent age-induced cancellous bone loss

Analysis of cancellous bone microarchitecture by μCT revealed that 6-month-old Cx43^{OT} mice exhibited increased trabecular thickness (Tb.Th) in the lumbar vertebra, without changes in the other trabecular bone parameters (Fig. 5*A*). Consistent with the increases in vertebral cancellous bone detected by μCT, vertebral compression testing detected increases in ultimate load/stress in the Cx43^{OT} compared with WT mice at 6 months of age (Fig. 5*B*). However, by 14 months of age, differences in cancellous bone between the two genotypes were no longer detected. Moreover, although aging led to a loss of vertebral cancellous bone BV/TV and Tb.N in both genotypes, decreases in vertebral Tb.Th were only detected in the 14-month-old Cx43^{OT} mice (Fig. 5*A*). Further, stiffness/modulus of the vertebra were decreased in aged mice from both genotypes, whereas decreases in ultimate load/stress were only detected in the 14-month-old Cx43^{OT} mice (Fig. 5*B*).

Consistent with the decreases in vertebral cancellous bone observed with aging in both WT and trangenic mice, histomorphometric analysis revealed decreases in MS/BS and BFR/BS (Fig. 6*A*) along with reductions in osteoblast number (N.Ob/BS) and surface (Ob.S/BS) (Fig. 6*B*) in the aged compared with young mice of both genotypes. Further, osteoclast parameters, N.Oc/BS, Oc.S/BS, and ES/BS, were higher in both genotypes at 14-month-old compared with 6-month-old mice. At 6 months of age, cancellous MAR and BFR/BS were reduced (Fig. 6*A*) and Ob.S/BS was decreased along with a tendency toward decrease in N.Ob/BS (Fig. 6*B*) in Cx43^{OT} mice compared with WT mice. At 14 months of age, MAR was still decreased in Cx43^{OT} compared with WT mice, whereas no differences in N.Ob/BS or Ob.S/BS were detected. On the other hand, no changes in osteoclasts were detected between the genotypes at either age (Fig. 6*C*). Taken together, these pieces of evidence suggest that increased osteocytic Cx43 does not prevent and may actually enhance cancellous bone loss induced with aging.

Discussion

Previous work from our laboratory demonstrated that Cx43 is critical for osteocyte survival and removal of osteocytic Cx43 leads a skeletal phenotype similar to that observed in aging with increases in osteocyte apoptosis and enhanced osteoclast recruitment, as well as deficits in the material properties of the cortical bone.[13,16] In this study, we examined the contribution of osteocytic Cx43 to the skeletal phenotype of aged mice, using Cx43^{OT} mice expressing a Cx43 transgene targeted to DMP1-8kb-expressing cells. We show that the prevalence of apoptotic osteocytes was significantly reduced in the cortical and to a lesser extent in the cancellous bone of 14-month-old Cx43^{OT} compared with WT mice, further demonstrating the critical role of Cx43 in maintaining osteocyte viability. In addition, we found that in aged Cx43^{OT} mice, reductions in osteocyte apoptosis were accompanied by changes in bone remodeling with increased

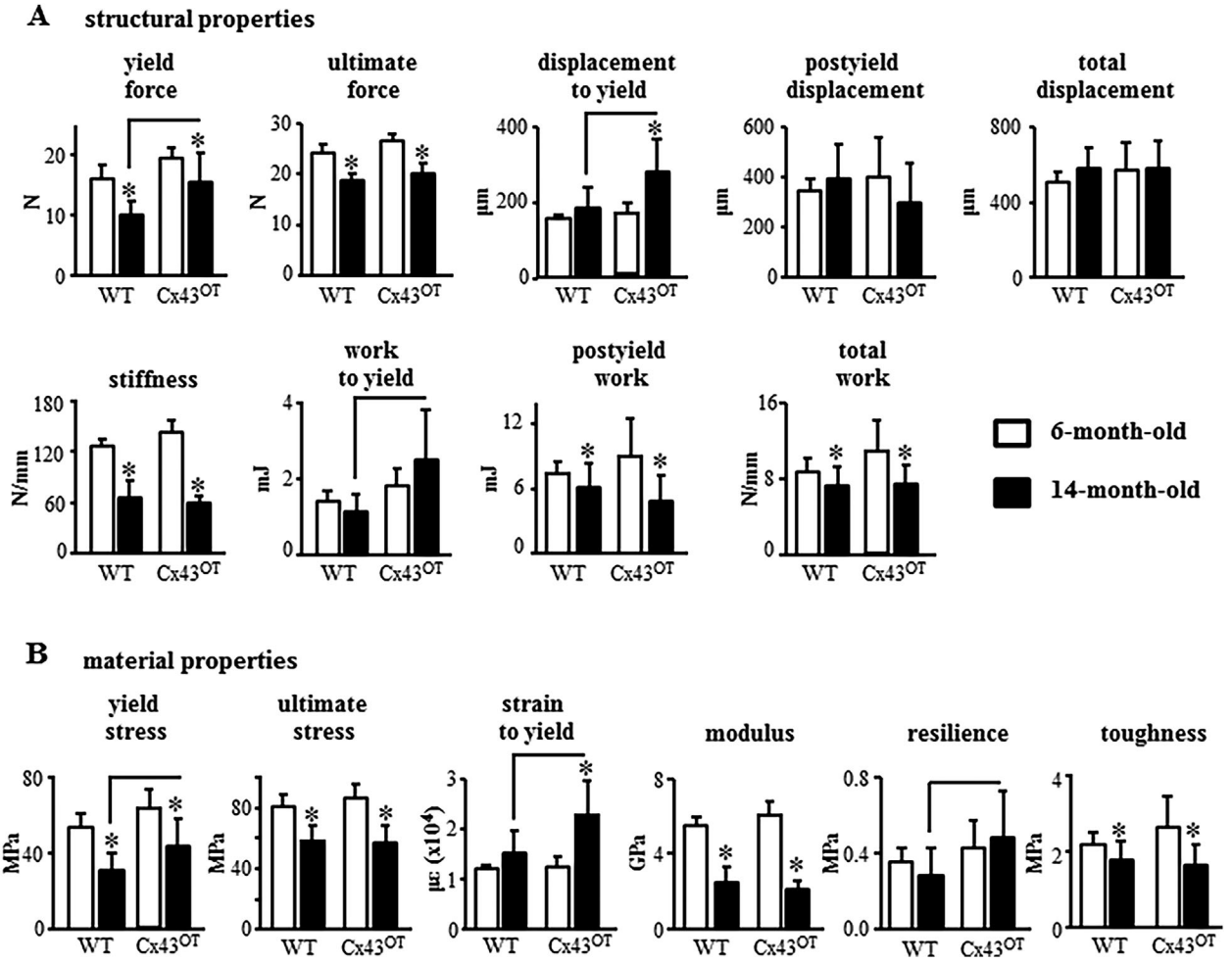

Fig. 4. Cx43^{OT} mice exhibit increased cortical bone resilience to fracture that is maintained with advanced age. Cortical bone biomechanical properties structural (*A*) and material (*B*) were evaluated by femoral 3-point bending testing. Six-month-old mice: $n = 7$ WT and $n = 5$ Cx43^{OT}, 14-month-old mice: $n = 11$ WT and $n = 8$ Cx43^{OT}. Bars represent mean ± SD, $^{*}p < 0.05$, versus 6-month-old genotype-matched mice by two-way ANOVA, Tukey, black line: $p < 0.05$, versus old control mice by *t* test.

formation and decreased resorption along the endocortical bone surface. Although this did not alter long bone geometrical changes induced with aging, improvements in the cortical mechanical properties were observed at the material level. It is possible that the aging process has just started in our 14-month-old animals, and although changes were detected at the cellular levels, we did not allow enough time for these alterations to translate into structural changes. Consistent with this possibility, we did not detect increases in bone mass in the aged compared with the young Cx43^{OT} mice by BMD or μCT analyses, even though the circulating markers suggest higher bone mass in the older animals. The reason for this discrepancy is not clear. However, it is possible that because the aging process may have just started in our animals and although changes were detected at the cellular levels, we did not allow enough time for these alterations to translate into structural changes. Furthermore, we cannot rule out the possibility that the moderate expression of the transgene in osteocytes and a potential uneven expression in femoral versus vertebral bone may provide some explanation for the weak bone mass phenotype of Cx43^{OT} mice.

In contrast, despite the increases in cancellous bone at 6 months of age in the Cx43^{OT} compared with WT mice and maintenance of spinal BMD at 9.5 months, age-induced cancellous bone losses were not prevented in the Cx43^{OT} mice by 14 months of age. These findings are consistent with previous reports demonstrating that removal of osteocytic Cx43 does not alter cancellous bone.[16] All together, our data demonstrate that Cx43 maintains osteocyte viability in both cortical and cancellous bone and that preservation of osteocyte viability appears to be critical for the maintenance of cortical bone quality in aging, although cancellous bone is still lost. Furthermore, increased Cx43 expression in osteocytes partially ameliorates the age-induced skeletal changes by preserving bone turnover, which likely improves cortical bone mechanical properties but does not prevent against cancellous bone loss in old age.

Bone fragility in aging individuals results not only from the loss of bone mass but also from deficits in bone quality.[5] The findings of the present study highlight the essential role of Cx43 in preserving osteocyte viability and maintaining the bone

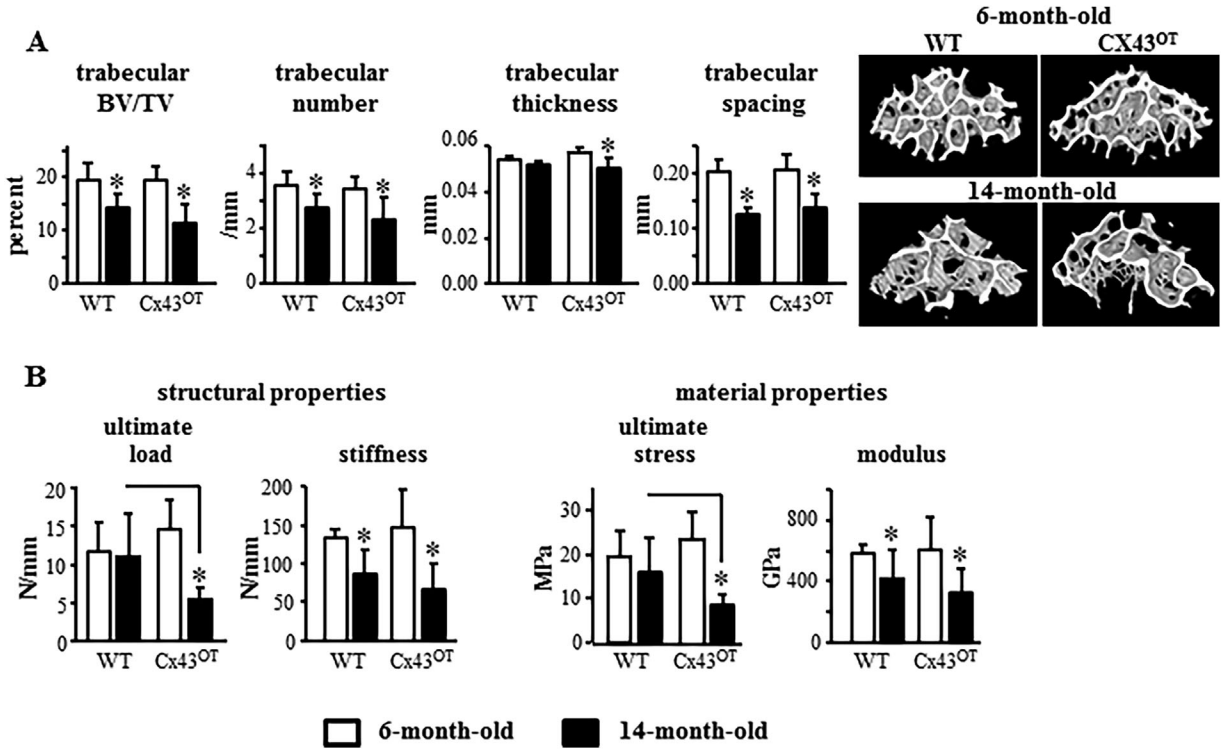

Fig. 5. Cx43^{OT} mice are not protected against age-induced loss of cancellous bone mass. (*A*) Cancellous bone microarchitecture was evaluated by μCT in the distal femur L_4 vertebra. Six-month-old mice: $n = 7$ WT and $n = 5$ Cx43^{OT}, 14-month-old mice: $n = 14$ WT and $n = 11$ Cx43^{OT}. Representative reconstructed 3D μCT images are shown. (*B*) Mechanical testing of the structural and material properties was evaluated by axial compression on the L_4 vertebra. Six-month-old mice: $n = 7$ WT and $n = 7$ Cx43^{OT}, 14-month-old mice: $n = 13$ WT and $n = 10$ Cx43^{OT}. Bars represent mean ± SD, $^*p < 0.05$, versus 6-month-old genotype-matched mice by two-way ANOVA, Tukey, black line: $p < 0.05$, versus old control mice by *t* test.

mechanical properties in aging. Age-related declines in bone material properties are accompanied by changes in the distribution and architecture of the cortical and trabecular bone.[6] We found that both aged WT and Cx43^{OT} mice exhibited the expected age-related increases in long bone diameter accompanied by decreases in BA/TA and cortical thickness. These changes in microarchitecture led to a decrease in the biomechanical properties of the bone at both the structural and material level. On the other hand, although decreases in the material properties were detected in the aged compared with skeletally mature WT mice, aged Cx43^{OT} mice partially maintained these biomechanical properties at both the structural and material level, when compared with the 6-month-old mice. Further, pre-yield mechanical measurements were all increased in aged Cx43^{OT} compared with aged WT mice. Interestingly, the pre-yield properties of the cortical bone in mice lacking osteocytic Cx43 were also reduced at both the structural and material level, whereas deficits in bone post-yield properties were only detected at the material level.[13] Based on the fact that we did not detect differences in cortical bone mass or geometry between the two genotypes at 14 months of age, it is reasonable to speculate that the increases in the structural and material properties in the 14-month-old Cx43^{OT} mice are not due to changes in bone architecture but are likely due to other factors at the level of the collagen/mineral. Thus, it is possible that the enhanced capability of the cortical bone of aged Cx43^{OT} mice to resist damage is due to changes in bone material as a result of increased osteocyte viability.

Bone quality depends not only on the geometry and microarchitecture of the bone but also on its material composition.[1,2] Bone material properties include mineral content, collagen composition, and microdamage accumulation.[1] Numerous studies have demonstrated the critical role that osteocytes play in sensing mechanical stimuli and coordinating targeted bone remodeling to repair damaged areas.[7,32] Decreases in osteocyte viability have been observed in many conditions underlying bone loss.[9] However, the specific mechanisms by which viable osteocytes prevent bone fragility in aging are not known. In the current study, we found that maintenance of osteocyte viability in the 14-month-old Cx43^{OT} mice is associated with preserved cortical bone elastic material properties and an improved resilience.

Preliminary gene expression measurements showed that increased expression of Cx43 in osteocytes results in higher levels of keratocan (a proteoglycan) in osteocytic cells (Fig. 1*A*) and, not shown, Chsy1 (a glucosaminoglycan) and Lox (lysil oxidase, an enzyme involved in collagen maturation) in bone preparations. Interestingly, deletion of Cx43 from osteocytic cells results in decreased levels of Lox,[13] suggesting that, as with the biomechanical properties, Cx43 deletion and overexpression leads to opposite effects on collagen-related genes. Further studies are needed to understand the mechanism for the changes in the material properties of the bone of mice expressing DMP1-Cx43. In addition, whether the improved ability of the bone to resist damage is due to prevention of microdamage accumulation

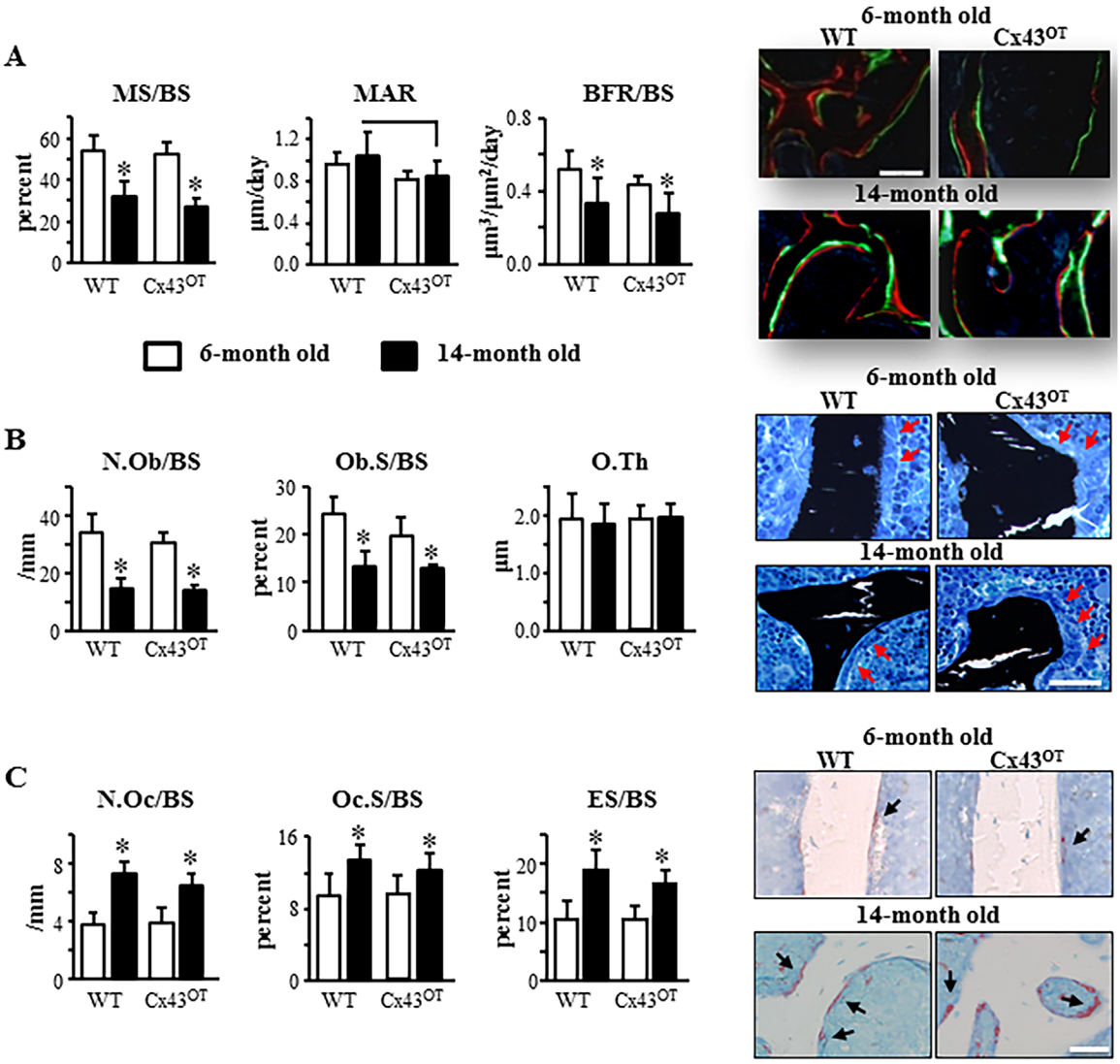

Fig. 6. Expression of osteocytic Cx43 does not alter changes in cancellous osteoblast or osteoclast activity induced with aging. (*A*) Vertebral cancellous bone MS/BS, MAR, and BFR/BS were measured in unstained longitudinal vertebral sections. Six-month-old mice: $n = 9$ WT and $n = 7$ Cx43^{OT}, 14-month-old mice: $n = 8$ WT and $n = 8$ Cx43^{OT}. Representative images show green and red fluorochrome levels. (*B*) N.Ob/BS, Ob.S/BS, and O.Th were scored in lumbar vertebra sections stained with von Kossa/McNeal. Six-month-old mice: $n = 9$ WT and $n = 8$ Cx43^{OT}, 14-month-old mice: $n = 7$ WT and $n = 7$ Cx43^{OT}. Representative osteoblast images are shown (arrow, red). (*C*) Cancellous osteoclasts were scored in TRAP/Toluidine blue-stained vertebral bone sections. N.Oc/BS, Oc.S/BS, and ES/BS are reported. Six-month-old mice: $n = 10$ WT and $n = 8$ Cx43^{OT}, 14-month-old mice: $n = 7$ WT and $n = 8$ Cx43^{OT}. Representative osteoclast images are shown (arrow, black). Bars represent mean ± SD, $^{*}p < 0.05$, versus 6-month-old genotype-matched mice by two-way ANOVA, Tukey, black line: $p < 0.05$, versus old control mice by *t* test. Scale bars = 100 μm.

or direct preservation of the bone material by living osteocytes or a combination of both remains to be determined.

Findings from numerous studies have consistently shown the differential role of osteocytic Cx43 in the cortical and cancellous bone compartments.[12] Removal of Cx43 from mature osteoblasts and osteocytes or exclusively from osteocytes results in cortical bone changes but does not alter cancellous bone.[13,16] Further, other studies have shown that expression of a truncated Cx43 lacking the c-terminus domain can negatively affect cancellous bone, whereas heterozygous deletion of Cx43 improves cancellous bone.[20,33] Our findings that osteocyte-targeted Cx43 transgene expression was sufficient to reduce osteocyte apoptosis in the cortical and to a lesser extent in the cancellous bone compartments, whereas changes in bone turnover and improvements in the mechanical properties of the bone were only observed in cortical bone, further demonstrate the differential actions of Cx43 in the two bone compartments.

In summary, the findings from the current study further highlight the critical role osteocytes play in the maintenance of cortical bone structure and mechanical properties in aging and demonstrate the requirement of Cx43-mediated actions in osteocytes for the preservation of osteocyte viability and cortical bone quality in aging. On the other hand, osteocytic Cx43 does not appear to play a critical role in maintaining cancellous bone in aged mice.

Disclosures

Authors have no conflict of interest.

Acknowledgments

The authors thank Drew Brown for his help with μCT analysis and Padmini Deosthale for her help with tissue acquisition. This research was supported by the National Institutes of Health R01-AR053643 to LIP. HMD and MWA are supported by an NIH T32-AR065971 grant. AAP is supported by an NIH Research Supplement to Promote Diversity in Health-Related Research (3R01AR067210-03S1). RPC received a scholarship from Coordination of Improvement of Higher Level Personnel (CAPES), Brazil (PDE# 232636/2014-1). EGA and CH received a scholarship from IUPUI, Life-Health Sciences Internship Program. AM, KA, and SV were supported by the CTSI summer scholars program at IUPUI. DL was supported by the IUSM SRPinAM: T-35 NIH training grant.

Authors' roles: Study design was performed by HMD and LIP. Data acquisition was performed by HMD, AAP, RPC, KA, SV, CH, EA, AM, and DL. SEH and MAH generated the transgene used to generate the mice. Advice on μCT analysis and biomechanical testing and contribution of materials was performed by MWA and MA. Data analysis and interpretation was performed by HMD, TB, and LIP. Manuscript was written by HMD and LIP. All authors revised the manuscript and approved the final version.

References

1. Fyhrie DP, Christiansen BA. Bone material properties and skeletal fragility. Calcif Tissue Int. 2015;97:213–28.
2. Zimmermann EA, Schaible E, Bale H, et al. Age-related changes in the plasticity and toughness of human cortical bone at multiple length scales. Proc Natl Acad Sci U S A. 2011;108:14416–21.
3. Jilka RL, O'Brien CA. The role of osteocytes in age-related bone loss. Curr Osteoporos Rep. 2016;14:16–25.
4. Almeida M, Han L, Martin-Millan M, et al. Skeletal involution by age-associated oxidative stress and its acceleration by loss of sex steroids. J Biol Chem. 2007;282:27285–97.
5. Chen H, Zhou X, Fujita H, Onozuka M, Kubo KY. Age-related changes in trabecular and cortical bone microstructure. Int J Endocrinol. 2013;2013:213234.
6. Ferguson VL, Ayers RA, Bateman TA, Simske SJ. Bone development and age-related bone loss in male C57BL/6J mice. Bone. 2003;33:387–98.
7. Bonewald LF. The amazing osteocyte. J Bone Miner Res. 2011;26:229–38.
8. Plotkin LI, Bellido T. Osteocytic signalling pathways as therapeutic targets for bone fragility. Nat Rev Endocrinol. 2016;12:593–605.
9. Tiede-Lewis LM, Xie Y, Hulbert MA, et al. Degeneration of the osteocyte network in the C57BL/6 mouse model of aging. Aging (Albany NY). 2017;9(10):2190–208.
10. Civitelli R, Beyer EC, Warlow PM, et al. Connexin43 mediates direct intercellular communication in human osteoblastic cell networks. J Clin Invest. 1993;91:1888–96.
11. Kato Y, Windle JJ, Koop BA, Mundy GR, Bonewald LF. Establishment of an osteocyte-like cell line, MLO-Y4. J Bone Miner Res. 1997;12:2014–23.
12. Plotkin LI, Bellido T. Beyond gap junctions: connexin 43 and bone cell signaling. Bone. 2013;52:157–66.
13. Bivi N, Nelson MT, Faillace ME, et al. Deletion of Cx43 from osteocytes results in defective bone material properties but does not decrease extrinsic strength in cortical bone. Calcif Tissue Int. 2012;91:215–24.
14. Lloyd SA, Loiselle AE, Zhang Y, Donahue HJ. Connexin 43 deficiency desensitizes bone to the effects of mechanical unloading through modulation of both arms of bone remodeling. Bone. 2013;57:76–83.
15. Plotkin LI, Lezcano V, Thostenson J, et al. Connexin 43 is required for the anti-apoptotic effect of bisphosphonates on osteocytes and osteoblasts in vivo. J Bone Miner Res. 2008;23:1712–21.
16. Bivi N, Condon KW, Allen MR, et al. Cell autonomous requirement of connexin 43 for osteocyte survival: consequences for endocortical resorption and periosteal bone formation. J Bone Miner Res. 2012;27:374–89.
17. Kalajzic I, Braut A, Guo D, et al. Dentin matrix protein 1 expression during osteoblastic differentiation, generation of an osteocyte GFP-transgene. Bone. 2004;35:74–82.
18. Tong D, Li TY, Naus KE, Bai D, Kidder GM. In vivo analysis of undocked connexin43 gap junction hemichannels in ovarian granulosa cells. J Cell Sci. 2007;120:4016–24.
19. Dutta S, Sengupta P. Men and mice: relating their ages. Life Sci. 2016;152:244–8.
20. Pacheco-Costa R, Davis HM, Sorenson C, et al. Defective cancellous bone structure and abnormal response to PTH in cortical bone of mice lacking Cx43 cytoplasmic C-terminus domain. Bone. 2015;81:632–43.
21. Bivi N, Pacheco-Costa R, Brun LR, et al. Absence of Cx43 selectively from osteocytes enhances responsiveness to mechanical force in mice. J Orthop Res. 2013;31:1075–81.
22. Tu X, Delgado-Calle J, Condon KW, et al. Osteocytes mediate the anabolic actions of canonical Wnt/b-catenin signaling in bone. Proc Natl Acad Sci U S A. 2015;112:E478–86.
23. O'Brien CA, Plotkin LI, Galli C, et al. Control of bone mass and remodeling by PTH receptor signaling in osteocytes. PLoS One. 2008;3:e2942.
24. Bellido T, Ali AA, Gubrij I, et al. Chronic elevation of PTH in mice reduces expression of sclerostin by osteocytes: a novel mechanism for hormonal control of osteoblastogenesis. Endocrinology. 2005;146:4577–83.
25. Plotkin LI, Bivi N, Bellido T. A bisphosphonate that does not affect osteoclasts prevents osteoblast and osteocyte apoptosis and the loss of bone strength induced by glucocorticoids in mice. Bone. 2011;49:122–7.
26. Pacheco-Costa R, Hassan I, Reginato RD, et al. High bone mass in mice lacking Cx37 due to defective osteoclast differentiation. J Biol Chem. 2014;289:8508–20.
27. Bouxsein ML, Boyd SK, Christiansen BA, et al. Guidelines for assessment of bone microstructure in rodents using micro-computed tomography. J Bone Miner Res. 2010;25:1468–86.
28. Dempster DW, Compston JE, Drezner MK, et al. Standardized nomenclature, symbols, and units for bone histomorphometry: a 2012 update of the report of the ASBMR Histomorphometry Nomenclature Committee. J Bone Miner Res. 2013;28:2–17.
29. Allen MR, Reinwald S, Burr DB. Alendronate reduces bone toughness of ribs without significantly increasing microdamage accumulation in dogs following 3 years of daily treatment. Calcif Tissue Int. 2008;82:354–60.
30. Sato AY, Cregor M, Delgado-Calle J, et al. Protection from glucocorticoid-induced osteoporosis by anti-catabolic signaling in the absence of Sost/sclerostin. J Bone Miner Res. 2016;31:1791–802.
31. Weinstein RS, Manolagas SC. Apoptosis and osteoporosis. Am J Med. 2000;108:153–64.
32. Nakashima T, Hayashi M, Fukunaga T, et al. Evidence for osteocyte regulation of bone homeostasis through RANKL expression. Nat Med. 2011;17:1231–4.
33. Buo AM, Tomlinson RE, Eidelman ER, Chason M, Stains JP. Connexin43 and Runx2 interact to affect cortical bone geometry, skeletal development, and osteoblast and osteoclast function. J Bone Miner Res. 2017;32:1727–38.